diagrams in Fig. 3 becomes

$$-\frac{16\pi^2}{E_0}\Big[\frac{c^6m^{*2}}{9}-\frac{2K_2K_3}{E_0^2}+\frac{c^4m^*}{2E_0}\Big(\frac{K_3}{K_2}+\frac{K_2}{K_3}\Big)+\frac{c^7m^{*2}}{6}\times\Big(\frac{1}{K_2}+\frac{1}{K_3}\Big)+\frac{c^4m^*}{2\pi}\Big\{\frac{4}{E_0}+\Big(\frac{4C}{E_0^2}+\frac{B}{E_0}\Big)C^{-1/2}\tan^{-1}\frac{2C^{1/2}}{B}+\Big(\frac{4C'}{E_0^2}+\frac{B'}{E_0}\Big)C'^{-1/2}\tan^{-1}\frac{2C'^{1/2}}{B'}\Big\}\Big], \quad (15)$$

where

$$K_2=c^2\{P_2^2+m^*(2A-E(k)-E(a)+E_0)\}^{1/2},$$
$$K_3=c^2\{P_3^2+m^*(2A-E(l)-E(b)+E_0)\}^{1/2},$$
$$B=(1/m^*c^4)(K_2^2-K_3^2)+E_0,$$
$$B'=(1/m^*c^4)(K_3^2-K_2^2)+E_0,$$
$$C=(1/m^{*2}c^8)(K_3^2-m^*c^4E_0)K_2^2,$$
$$C'=(1/m^{*2}c^8)(K_2^2-m^*c^4E_0)K_3^2. \quad (16)$$

Since the most important matrix elements of the hard core in the first G matrix give relative momenta $k_a=k_b=\pi/2c$ it is reasonable to take the initial relative momenta in G_2 and G_3 equal to $k_1=\pi/4c$. In this case

$$E_0=(4k_1^2/m)+2A. \quad (17)$$

We simplify further by taking $A=0$ and $m^*=1$, since these parameters are not well established. The values of various expressions with this choice of parameters are given in Table I, both for the core volume term alone [the first part of (2)] and for all of G^R. The first row gives the Goldstone contribution, expression (8), which one hopes the Hartree-Fock potential will cancel. The second row gives the residual contribution as given by (14) or (15) of this paper. When the second row is small, as it is when all of G^R is used, the H-F potential is serving its function even in 4th order. When the second row is of the same order as the first, as with the core volume term, the H-F potential which cancelled the third-order diagrams exactly is not qualitatively decreasing the fourth-order diagrams.

TABLE I. Values of various expressions in the text.

	Core volume term only	All of expression (2)
Goldstone contribution (8)	$-14.2c^8$	$-220\ c^8$
Residue, i.e., (14) or (15)	$-7.1c^8$	$-16.3c^8$

Although the illustration may be somewhat artificial, since, as can be seen from the table, the core volume term is only a small part of the total hard-core contribution; it has been the purpose of this paper to show that rapid convergence of the Goldstone series is by no means assured by making the third-order diagrams small.

ACKNOWLEDGMENT

The author is grateful to the Physics Division of the Aspen Institute for Humanistic Studies for extending their hospitality while some of this work was done.

PHYSICAL REVIEW VOLUME 133, NUMBER 6B 23 MARCH 1964

Average Number of Prompt Neutrons from U^{235} Fission Induced by Neutrons from Thermal to 8 MeV

D. S. MATHER, P. FIELDHOUSE, AND A. MOAT
Atomic Weapons Research Establishment, Aldermaston, Berks, England

(Received 21 October 1963)

A large, loaded-liquid scintillation counter has been used to measure the average number, $\bar{\nu}$, of neutrons emitted in the neutron-induced fission of U^{235} as a function of the incident energy. Time-of-flight techniques were employed where necessary to select fissions induced by neutrons of the desired energy. Values at nineteen energies in the range thermal to 8 MeV were determined; absolute values are based on $\bar{\nu}$ (Cf^{252}, spontaneous) $=3.782\pm0.024$, relative errors are about 1%. The variation of $\bar{\nu}$ with energy cannot be represented by a single straight line. A satisfactory fit to the experimental points is given either by the relationship

$$\bar{\nu}(E)=(2.423\pm0.008)+(0.088\pm0.008)E+(0.0088\pm0.0011)E^2,$$

or by two straight lines

$$\bar{\nu}(E)=(2.418\pm0.008)+(0.109\pm0.006)E \text{ from 0 to 3 MeV},$$
$$\bar{\nu}(E)=(2.200\pm0.023)+(0.181\pm0.005)E \text{ from 3 to 8 MeV}.$$

I. INTRODUCTION

THE measurement of $\bar{\nu}$, the average number of neutrons emitted in fission, is important from both the practical and theoretical viewpoints. Calculations of the properties of fissile assemblies require precise knowledge of $\bar{\nu}$, while any proposed theory of fission must show how this parameter is related to the excitation, mass, and charge of the fissioning nucleus.

A table of $\bar{\nu}$ for different nuclides is given by Leachman[1] and some later values are contained in a review by Safford and Havens.[2] A recent compilation by Asplund-Nilsson[3] lists published values of spontaneous and neutron-induced fission for many fissile nuclides. In general, a comparison is made with some standard value, the most usual being $\bar{\nu}$ for thermal fission of U^{235}; the use of a spontaneous fission $\bar{\nu}$ such as that for Cf^{252} appears to offer some advantages. The neutron-induced fission of U^{235} has been investigated most thoroughly and early results showed that $\bar{\nu}$ increases with increasing incident-neutron energy (E). Because of a lack of accurate results it was usual to assume a linear variation of $\bar{\nu}$ with E from thermal to 14 MeV, with a slope $d\bar{\nu}/dE$ of about 0.13 MeV^{-1}. However, more recent results of improved accuracy and better energy coverage[4–6] suggest that the dependence of $\bar{\nu}$ on E may not be as simple as this. (See Table VII.)

The work reported here is a continuation of that described previously.[7] Details were given of the measurement of Cf^{252} spontaneous fission $\bar{\nu}$ with respect to the Harwell Pu^{240} standard source and of how a Cf^{252} sample was then used to calibrate the neutron-detection efficiency of a large loaded-liquid scintillation counter. Measurements made with that calibrated counter included $\bar{\nu}$ for U^{235} fission induced by neutrons of 75 keV, 2.5 MeV and 14.2 MeV. For the work presented here, a larger and more efficient counter was used to make measurements covering the range thermal to 8 MeV. Because it is essential to know the energy of the neutrons producing fissions, the energy spectrum of neutrons at the position of the fission chamber was measured by conventional time-of-flight methods. For primary-neutron energies above 4 MeV, time-of-flight selection was an intrinsic function of the $\bar{\nu}$ recording equipment. Most of the results from 40 keV to 3 MeV were given previously.[6]

II. EXPERIMENTAL METHOD

A. Outline of Method

The neutron detector is a large volume of loaded-liquid scintillator which gives a high efficiency for detecting neutrons emitted in fission. Neutrons entering the organic scintillator lose most of their energy in hydrogen recoils within a few nanoseconds and then diffuse in the liquid for a few microseconds until captured randomly in time by the material used to load the scintillator. The capture γ rays produce scintillations, mainly by the Compton effect, the light due to separate γ rays from a single capture combining to form a single pulse in the photomultipliers. If a fission chamber is placed at the center of the counter then a "prompt" scintillation pulse is produced at the time of a fission event, the pulse being caused by fission γ rays, and the most energetic hydrogen recoils. The associated electronics is so arranged that a pulse from the fission chamber, if in coincidence with a prompt pulse from the scintillator, can open an electronic "gate" of several tens of microseconds duration which permits the counting of all scintillation pulses except the prompt pulse.

Calibration of the detector efficiency was carried out by placing a chamber containing spontaneously fissile Cf^{252} at the center of the counter, measuring the number of capture pulses (i.e., number of detected neutrons) per fission and comparing this with the standard $\bar{\nu}$ value, 3.782, for spontaneous fission of Cf^{252}. A fission chamber containing U^{235} was then substituted for the Cf^{252} and a collimated beam of neutrons used to induce fission in the U^{235}. The measured number of capture pulses per fission divided by the detector efficiency yielded the value of prompt $\bar{\nu}$ at the energy of the incident neutrons.

B. The Neutron Detector

The scintillation counter is spherical with a diameter of 76 cm and contains approximately 240 liters of Gd-loaded liquid.[8] Gadolinium was chosen as the loading element in preference to cadmium because its higher capture cross section for neutrons in the thermal region enables the same efficiency to be obtained using much smaller concentrations (0.5% by weight) and this in turn allows the liquid to retain its good pulse height and transmission characteristics. A thin-walled, cylindrical tube of 6.5 cm diam runs diametrically through the counter allowing a fission chamber to be placed at the center.

Twelve 5-in.-diam photomultipliers, EMI-type 9618A, are fitted around the surface of the sphere with their photocathodes in direct contact with the liquid; the total area of the photocathodes is more than 6% of the surface area of the counter. The photomultipliers are connected electrically as three banks each of four tubes, the tubes of a single bank being arranged so that approximately isotropic coverage of the whole volume is achieved. Each photomultiplier has its own "extra-high tension (e.h.t.)" supply and the signals from all the tubes in a bank are fed via short 100-Ω cables to a mixing network, the lengths of the cables being adjusted to allow for the different transit times of the tubes. From the mixing networks the signals from each bank pass through 200-Mc/sec distributed amplifiers to a three-

[1] R. B. Leachman, Proc. UN Intern. Conf. Peaceful Uses At. Energy, 2nd, Geneva **15**, 229 (1958).
[2] G. J. Safford and W. W. Havens, Nucleonics **17**, No. 11, 134 (1959).
[3] I. Asplund-Nilsson, Försvarets Forskningsanstalt Avdelning (Stockholm) 4 Rapport A 4290–411, 1963 (unpublished).
[4] D. Butler, S. Cox, J. Meadows, J. Roberts, A. Smith, and J. Whalen, Proc. IAEA Conf. Physics of Fast and Intermediate Reactors **1**, 125 (1962).
[5] B. C. Diven and J. C. Hopkins, Proc. IAEA Conf. Physics of Fast and Intermediate Reactors **1**, 149 (1962).
[6] A. Moat, D. S. Mather and P. Fieldhouse, Proc. IAEA Conf. Physics of Fast and Intermediate Reactors **1**, 139 (1962).
[7] A. Moat, D. S. Mather and M. H. McTaggart, Reactor Sci. and Technol. (J. Nuclear Energy Parts A/B) **15**, 102 (1961).
[8] Type Ne313, Nuclear Enterprises, Ltd., Great Britain.

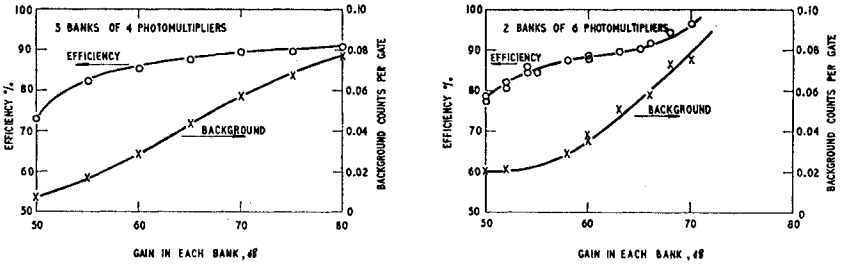

FIG. 1. Variation of counter efficiency and background with amplifier gain in each bank of photomultipliers, for two and three-bank arrangements.

fold coincidence unit. Using the photomultipliers in a coincidence system allows the individual tubes to be operated at high gains since very small genuine signals can be distinguished from noise thus making detection of weak scintillations possible and thereby increasing the efficiency. In addition, the effect of afterpulsing in the photomultipliers is greatly reduced. The variation of efficiency with amplifier gain in each bank (and also e.h.t.) has been measured and the results are shown graphically in Fig. 1. For comparison purposes, the curve of efficiency against gain for 2 banks of 6 tubes is also shown. The threefold arrangement was chosen in preference to the twofold because of the better plateau; this has a length of 20 db and a slope of 0.16% per db (equivalent to a slope of 7% per kV of e.h.t.). The tubes are normally operated at the low-gain end of the plateau since this gives sufficient stability of efficiency while reducing the background counting rate. Over several months the efficiency was found to be constant at about 89% within about 0.2%. The counter appears to be provided with sufficient photomultipliers since measurements of the efficiency made with only 3 tubes in each bank are only 1% lower.

C. Shielding System

The counter is used near intense neutron sources and because of its large sensitive volume it is essential to provide it with adequate shielding against neutrons coming directly from the source as well as room-

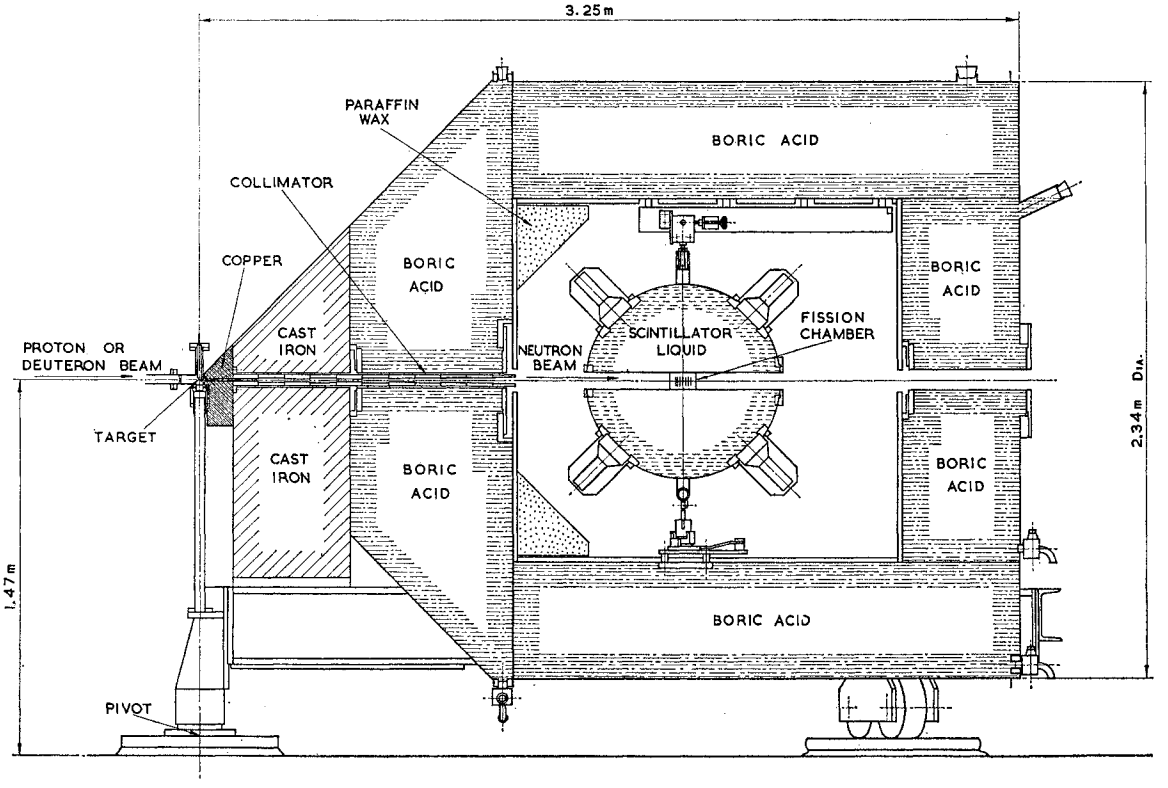

LIQUID SCINTILLATION COUNTER-SHIELDING SYSTEM

FIG. 2. Shielding and collimating system.

TABLE I. Details of neutron sources used for $\bar{\nu}$ measurements.

Mean neutron energy (MeV)	Reaction	Collimator angle	Pulsed beam	Gating rate per hour	Neutron energy spread Due to target keV	Due to angular width keV
Thermal	Li(p,n) +moderator	90°	no	6000	...	...
0.45[a]	Li(p,n)	0°	no	1000	55	...
0.15	Li(p,n)	0°	no	300	40	...
0.25	T(p,n)	100°	no	600	25	5
0.35	T(p,n)	76.2°	no	400	115	7
0.50	T(p,n)	72.5°	no	500	115	8
0.75	T(p,n)	43.25°	no	600	60 and 160	8
0.85–4.0	T(p,n)	5°	no	300–1200	70–190	1–4
4.0	D(d,n)	5°	no	1000	680	2
5.0–8.0	D(d,n)	5°	yes	400–600	200–400	4–8

[a] Two groups of neutrons 8–30 keV and 30–63 keV, mean energy 45 keV; mean energy of neutrons producing fissions, 40 keV.

scattered neutrons and general γ-ray background. In addition, it is necessary to provide a collimator to define a neutron beam directed at the fission chamber within the counter.

Figure 2 shows the arrangement of the shielding and collimating system. The charged-particle beam from the Aldermaston 6 MV Van de Graaff accelerator emerges vertically, is bent through 90° by an analyzing magnet and travels some 12 m down evacuated beam piping to the target which is the source of neutrons. This target is mounted above the pivot of the shield which can be rotated in the horizontal plane through all angles from the forward direction of 110° (see Sec. II E) with an additional position at 145°. Factors considered in designing the shield were discussed previously when a vertical system was described.[7] The present shield has a few extra features, namely:

(a) A copper nose piece to further reduce the transmission of high-energy neutrons.

(b) Loading of the water shield with boric acid so that neutrons are captured preferentially in boron, giving rise to γ rays of 480-keV energy, rather than in hydrogen where the capture γ rays are more energetic (2.2 MeV) and hence more penetrating.

(c) A 5-cm-thick lead wall inside the inner compartment of the shield between the cone and the counter to attenuate the γ rays from the copper, iron and water in the cone.

(d) Addition of a large iron block to the underside of the iron cone to prevent high-energy neutrons from the source reaching the counter after a single scatter in the concrete floor.

The charged particles from the Van de Graaff are focused by electrostatic strong-focusing lenses to give a narrow beam through a 2-mm-diam tungsten aperture before striking the target 10 cm beyond. Neutron beam collimation is such that the beam produced is 3 cm in diam at the position of the fission chamber within the counter.

D. Fission Chambers

Continuous-flow fission chambers were used with a gas mixture of 90% argon and 10% methane at atmospheric pressure. The Cf^{252} sample was deposited over a 3-cm-diam region on a thin platinum disk and gave about 80 fissions/sec. A multiplate chamber contained approximately 170 mg of U^{235} on sixteen plates separated by 0.3 cm and with a 3-cm-diam coating. The isotopic purity is given in Sec. III B5.

E. Source of Neutrons

Neutrons were produced by one of the following reactions: $Li^7(p,n)$, T(p,n), or D(d,n). The Li^7 was in the form of lithium fluoride while the deuterium and tritium were absorbed in titanium evaporated on to gold backings. Table I shows the reaction used in a particular energy range, the gating (or fission) rates obtained and the estimated total spread in neutron energy due to the thickness of the target and the angular width of neutron beam.

Background counts in the detector arise from scintillation-counter pulses which are unrelated to fission but which occur during the time the gate is open and hence are counted as fission neutrons. The current on target and therefore the gating rate was usually limited in order to keep the background counts below a certain level, normally 20% of the genuine counts per gate. On some occasions the maximum current available from the accelerator was the limiting factor rather than the background level. The accelerator was unable to provide high currents at energies less than 1.8 MeV and for bombarding energies below this it was often useful to select molecular beams H_2^+ of D_2^+ of twice the required proton or deuteron energy.

For all of the reactions used, there is peaking of neutron production in the forward direction. However, the smallest collimator angle used (except for the Li reactions) was 5°, since at 0° the collimator "looks" at the tungsten aperture and the beam piping which are

sources of unwanted neutrons when deuterons or high energy protons are the bombarding particles. Whenever possible the collimator was set at 5° and the accelerator energy was varied to give the appropriate neutron energy: For the low-energy neutrons from the $T(p,n)$ reaction it was necessary to swing the shield to angles as large as 100°. Thermal neutrons were obtained by surrounding the target with a 15 cm thickness of polyethylene and producing low-energy neutrons (45-keV mean) in a forward cone from $Li^7(p,n)$ induced by protons 8 keV above threshold. In order to minimize the number of neutrons of primary energy which enter the collimator, the target is observed at 90° through a 5-cm-diam hole. The effectiveness of the moderator was checked by measuring the gating rate with and without a 1-mm-thick Cd disk covering the end of the U^{235} fission chamber nearest the neutron source; the ratio was about 0.18:1.

F. Time of Flight

Neutrons having energies other than that required may be present causing spurious fissions and some neutron-energy-selection system may be necessary to ensure that results are not affected by these events. Time-of-flight techniques were called upon to help in solving these problems. There appear to be three main ways in which low-energy neutrons could arise. Firstly, the solid target which was the neutron source consisted of titanium, gold, and perhaps a carbon deposit in addition to the deuterium or tritium, so that unwanted neutrons could be produced at the target. Secondly, the necessity of neutron-beam collimation means that neutrons of primary energy could be degraded by one or two interactions in the surface regions of the collimator. Finally, some neutrons from the source or from the general room background might undergo many interactions and yet still get inside the shield and into the fission chamber. Allowance for some of the undesirable neutrons could be made by taking properly normalized blank target runs. However, these could not reproduce the exact fraction of neutrons due to carbon buildup on the target. A further objection is that at high energies only about 30% of the neutrons are of the required energy and very long runs would be required in order to yield accurate values for the differences in gated fissions and detected neutrons. For these reasons the present work relied on time-of-flight techniques rather than blank target subtraction methods.

Time of flight (TOF) was applied in three ways:

(a) To obtain an energy spectrum of neutrons at the position of the fission chamber (TOF spectra, Sec. II F2).

(b) To select for $\bar{\nu}$ measurement those fissions induced by neutrons having the flight time corresponding to neutrons of the required energy (TOF selection, Sec. II F3).

(c) To record the times of occurrence of fission events relative to the beam pulse. (Referred to as "fission-time sorting," Sec. II F4.)

Method (a) was used to look for groups of high-energy neutrons principally from the target backing, etc. If only the primary energy peak was observed, the $\bar{\nu}$ experiment could be carried out using a dc (i.e., unpulsed) neutron source. If additional neutron groups were present then method (b) had to be employed, the necessary time resolution being deduced from the TOF spectrum.

The detector used for the spectra measurements of method (a) had a low-energy cutoff at about 0.5 MeV and lower energy neutrons would be undetected although able to induce fissions. Thermal neutrons would be particularly troublesome in this respect. Fission-time sorting was devised to overcome this difficulty. The method gives essentially the same information as the TOF spectra with the advantage of responding to all neutron energies and enabling corrections for low-energy neutrons to be made to both dc and pulsed $\bar{\nu}$ measurements. The disadvantages are slower accumulation of data, poorer time resolution and ambiguities of neutron energy because the absence of an energy threshold prevents discrimination against neutrons from previous beam pulses. More details of the different methods are given below.

1. Beam Pulsing Arrangements

The beam was pulsed either in the top terminal of the Van de Graaff or by a post-acceleration deflection system. The latter method was used in connection with the earlier work up to 3 MeV: the ion source was a conventional rf type and the water-cooled deflection plates were 60-cm long and fed from a 2.5 Mc/sec crystal-controlled oscillator which also provided the "time-zero" signal via a pickup loop. This system gave rise to an appreciable background when used with deutrons or high-energy protons, but this background was considerably reduced when a top-terminal pulsing facility using a duoplasmatron ion source[9] became available. This was used for measurements between 5- and 8-MeV neutron energy. A time-zero was obtained by pickup from the accelerated-particle pulse by means of an aerial mounted about 50 cm in front of the target. This aerial consisted of a 2-cm-diam by 15-cm-long copper cylinder through which the beam passed. Connected to the aerial and close to it was a head unit comprising a 5 Mc/sec ringing oscillator which was heavily damped to avoid phase shift with respect to the beam-pulsing frequency and which fed a limiting amplifier giving a square-pulse output with a risetime of a few nanoseconds. Signals large enough to saturate this amplifier were necessary for satisfactory operation and

[9] Manufactured by High Voltage Engineering Corporation, Burlington, Massachusetts; see also J. Towle and W. B. Gilboy, Nucl. Phys. 44, 256 (1963).

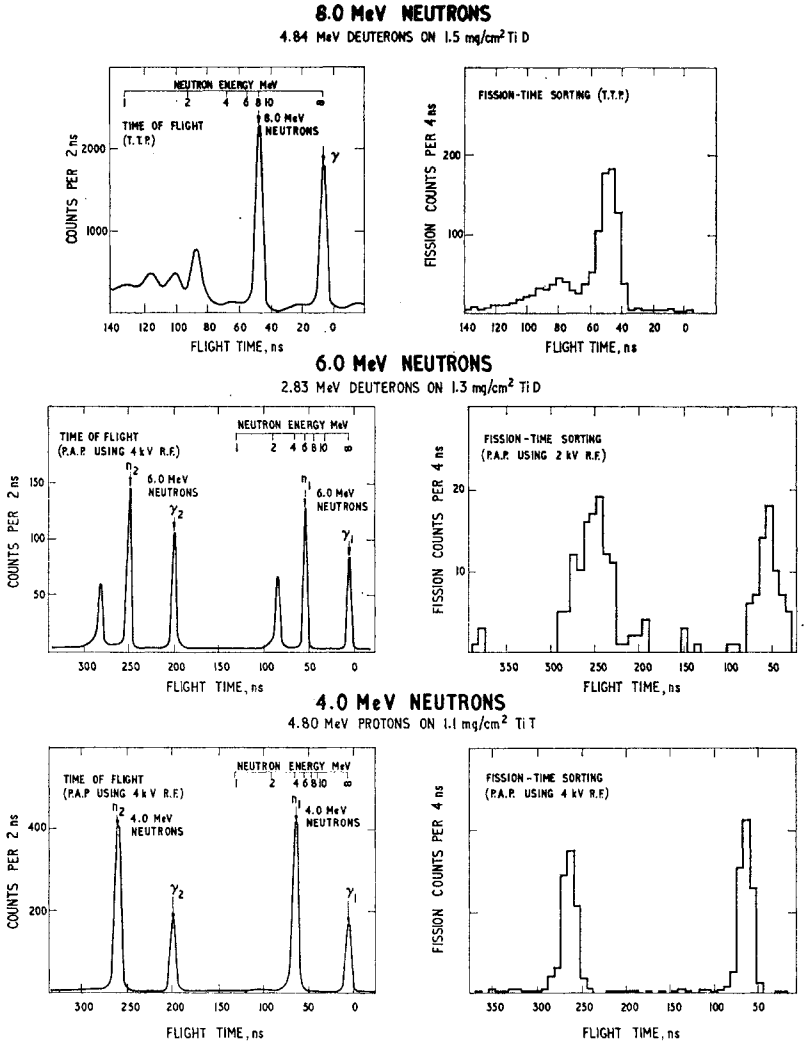

FIG. 3. Time-of-flight spectra and fission-time sorting displays for primary-neutron energies of 4, 6, and 8 MeV. (TTP, top-terminal pulsing; PAP, post-acceleration pulsing.)

could be obtained using mean beam currents in excess of 0.05 μA.

2. *Time-of-Flight Spectra*

A neutron detector consisting of a small plastic scintillator 3 cm diam by 0.8 cm thick on a Philips 50 AVP photomultiplier was placed at the center of the large scintillation counter and a time sorter (time to pulse-height converter) was used to display the time spectrum on a 400-channel pulse-height analyzer. The graphs on the left of Fig. 3 show spectra obtained for primary neutron energies of 4.0, 6.0, and 8.0 MeV. For primary neutron energies from 5.0 to 8.0 MeV it was clear that dc (unpulsed) measurements of $\bar{\nu}$ would be seriously in error since some fissions would be caused by the lower energy neutron groups. These groups are due to (d,n) or (p,n) reactions in the target materials (including possibly carbon) or to deuteron breakup. For primary energies up to nearly 5 MeV from the $T(p,n)$ reaction and with a time resolution of 6.5 nsec, no degraded neutrons were evident between the primary energy peak and 0.5 MeV. This lower energy limit was set by the pulse-height response of the plastic scintillator and noise arising in the photomultiplier tube.

3. *Time-of-Flight Selection*

A time-of-flight selection system was used for all $\bar{\nu}$ determinations where the neutron energy was 5 MeV or above. This system had to select for $\bar{\nu}$ measurements those fissions induced by neutrons in the primary energy group. Details of the electronics used are given in Sec. II G. The gate would not trigger unless a beam timing signal, after a suitable pre-set delay, arrived in coincidence with the prompt pulse from the scintillation counter (due mainly to γ rays from the fission). The value of the pre-set delay determined the energy selected.

The primary group of neutrons lies, in time, between

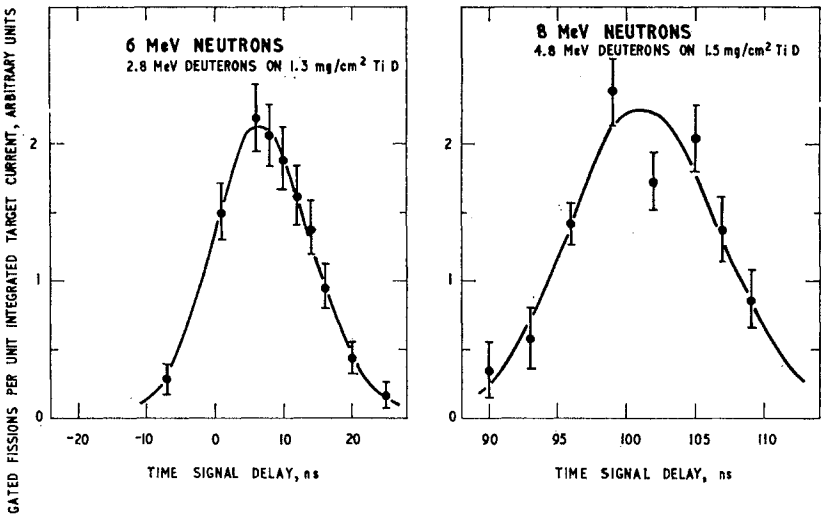

FIG. 4. Curves of gated fission rate versus beam-timing signal delay obtained with the time-of-flight selection system for 6- and 8-MeV primary neutron energies.

secondary neutron groups originating from consecutive beam bursts. The resolving time of such a coincidence system need only be sufficiently good to exclude secondary neutron groups: Beam-pulse widths considerably greater than the resolving time may be utilized[10] provided the delay can be set so that secondary neutron groups are excluded. Having met these conditions and thus isolated the primary group, the energy spread of the neutrons which induce the selected fissions is determined mainly by the target thickness and any effect due to the collimator; it is independent of the resolving time of the coincidence system and of the beam-pulse width. The energy spread of the primary group is discussed in Sec. III B4.

Figure 4 shows a plot of the gated fission rate as a function of timing signal delay for primary-neutron energies of 6 and 8 MeV; such curves enable the correct choice of delay to be made. In order to accumulate events as quickly as possible it is obviously desirable to work close to the peak, provided that by doing so no secondary neutron groups are included. For the measurements described, the peak was chosen as the operating point. Inspection of the above curves, together with the corresponding time-of-flight spectra, showed that in all cases up to 8 MeV this was a permissable procedure.

At higher energies, the secondary neutron group would no longer be excluded if the same coincidence resolving time were maintained but the primary group could again be isolated by reducing the pre-set delay by a few nanoseconds, thus moving the operating point from the position of peak gating rate.

[10] Any part of the beam pulse which lies outside the resolving time curve of the fast coincidence system is useless; that part of the beam pulse occurring nearest the peak of the curve has the best chance of producing a recordable fission. Consequently, the beam pulse would ideally be made short compared with the resolving time. This condition yields the lowest background and random fission rates (Sec. II F4) relative to the wanted fission rate. In practice, the lower mean beam current available at short pulse widths is likely to conflict with this ideal.

For measurements up to 7 MeV a beam-pulse width of 12 nsec was used; this was reduced to 4 nsec for the determination at 8 MeV. The coincidence resolving time was 18 nsec and it is interesting to note that this was attained with a 76-cm-diam counter not specifically designed for fast timing experiments. With 18 nsec resolving time and a beam-pulsing frequency of 5 Mc/sec (200 nsec between bursts) the time-of-flight selection system rejected 91% of fissions occurring randomly in time in addition to rejecting fissions due to neutron groups other than the primary. It did not eliminate those fissions, if any, induced by neutrons from previous beam pulses with flight times of $[N\times 200+(f\pm 9)]$ nsec, where N is an integer and f is the flight time of the primary neutrons.

4. *Fission-Time Sorting*

Since the method of Sec. II F2 is not sensitive to any neutrons below about 0.5 MeV, it was necessary to show that such neutrons were not causing a significant fraction of the observed fissions; for this, fission-time sorting was used. The plastic scintillation counter of the conventional time-of-flight apparatus, described in Sec. II F1, was replaced by the U^{235} fission chamber. The time sorter was started by a prompt pulse from the large scintillation counter, the appropriate fast pulse being "gated" by the slower pulse from the fission chamber and was stopped by the beam timing signal.

The right-hand graphs in Fig. 3 show typical fission-time sorting displays. The sharp peaks correspond to fissions induced by primary-energy neutrons. At primary energies below 5 MeV, all the fissions occurring between the peaks are assumed to be random and due to low-energy neutrons, i.e., less than 0.5 MeV. A dc measurement of $\bar{\nu}$ includes all this low-energy contamination but its estimation from the fission-time display is straightforward. The number R of random fissions per

primary fission is given by

$$R=\left(\frac{N_r}{t}\right)\left(\frac{N_p}{T}\right)^{-1},$$

and the fractional contamination is

$$\frac{RN_p}{N_p+RN_p}=\frac{N_rT}{N_pt+N_rT},$$

where T is the time between beam pulses (200 nsec); t is the time interval in the fission-time display which was scanned for random fissions; N_r is the total number of random fissions in time t; and N_p is the total number of fissions in the primary peak as given by the fission-time display.

For primary energies above 4 MeV, secondary neutron peaks become apparent and although time-of-flight selection eliminates these, gates due to a small fraction of the randomly occurring component will still be recorded. The quantity R, defined above, may be estimated from the number of fissions which occur during those intervals on the fission-time display for which no secondary peaks are discernible on the corresponding time-of-flight spectrum. The low-energy contamination, when using a pulsed beam, is then given by the dc contamination multiplied by the ratio of the fourfold resolving time to the interval between beam bursts (200 nsec). This fourfold resolving time is that of the fast coincidence unit for prompt scintillation pulses and the pulsed-beam timing signal (see Fig. 5) and is independent of beam burst width, being determined solely by the width of the threefold and beam timing signals. With the latter clipped to 10 nsec, the measured value of the resolving time was 18 nsec.

The measured contamination may contain fissions induced by neutrons of all energies below 0.5 MeV. Subsequent correction of $\bar{\nu}$, for pulsed or for dc measurements, is made on the assumption that all of these have $\bar{\nu}=\bar{\nu}$ (thermal); this may not be far from the truth because of the high weighting given by the thermal fission cross section. In a typical case, a 10% contribution from thermal fission would necessitate a correction of +1.8% in a dc determination of $\bar{\nu}$ at 4 MeV, and +0.3% in a pulsed measurement at 8 MeV.

G. Electronics

Figure 5 is a block diagram of the electronics used in the $\bar{\nu}$ experiments and also shows the arrangement used for fission-time sorting which could be run simultaneously when required. The functioning of the unit labeled "multiple-event analyzer" (designed by Gore[11]) was as follows. Each genuine fission event detected by the slow coincidence unit was arranged to open a gate of 40 μsec duration. Scintillation pulses from the threefold fast coincidence unit were passed through a discriminator in the multiple-event analyzer which had a dead time of 0.22 μsec. The output of this discriminator was fed to the input of the gate and also to the "background scaler"—a fast scaler which recorded the number of pulses being presented at the gate. Those scintillation pulses which got through the gate were converted to a standard pulse height and at the end of the gating period an output pulse proportional to the number of input pulses accumulated was delivered to the pulse-height analyzer. The pulse-height analyzer displayed the observed frequencies of multiplicities, i.e., the number of gates containing 0, 1, 2, ⋯, 9 counts. This information, together with the background scaler count and the duration of the experimental run, provided the data for the determination of $\bar{\nu}$.

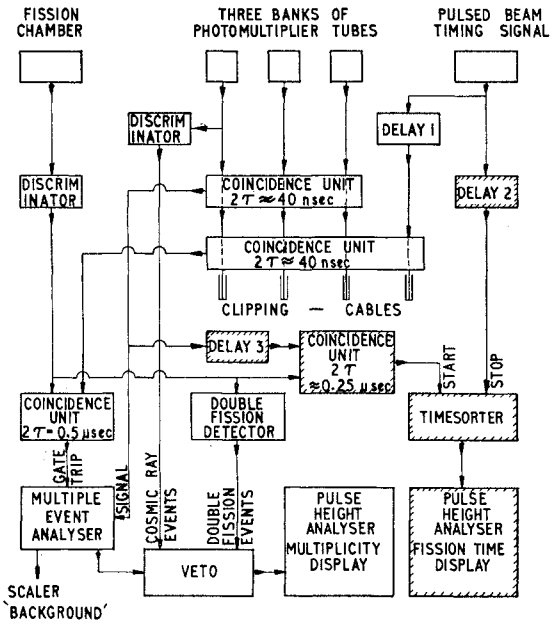

FIG. 5. Block diagram of electronics for combined $\bar{\nu}$ measurement and fission-time sorting. Units required for fission-time sorting are shown cross hatched.

H. Data Processing

The data were obtained in a series of short runs of 1- or 2-h length during which the background was held constant to ±10% by adjusting the current on target (see Sec. III B12). Runs to calibrate the counter efficiency with the Cf^{252} chamber lasted 10 min and were performed at the beginning and end of each day. It was necessary to correct the *observed* data for background and for dead-time losses in the multiple-event analyzer in order to obtain the *detected* frequencies of multiplicities. The Aldermaston IBM-7090 computer was programmed to simulate the counting electronics of the experiment; known combinations of genuine and background counts were repeatedly fed into the input, and the probabilities of certain numbers of counts appearing

[11] W. G. Gore, Nucl. Instr. Methods **7**, 320 (1960).

at the output were accumulated. After many such trials (10^4 per combination), a correction matrix of probability coefficients was obtained; this matrix characterizes certain properties of the counting experiment (gate length and input dead time of the multiple-event analyzer) and is valid as long as none of these properties is altered. To correct the results obtained in a $\bar{\nu}$ experiment, the matrix was put into the computer, together with the observed frequencies of multiplicities and the background rate, and then the probabilities A_n of detecting n fission neutrons were calculated. More details of this procedure were given in an earlier paper.[7]

The detector efficiency,

$$\epsilon=\frac{\sum_n n\,A_n(\mathrm{Cf}^{252})}{\bar{\nu}(\mathrm{Cf}^{252})},$$

and

$$\bar{\nu}(\mathrm{U}^{235})=\frac{\sum_n nA_n(\mathrm{U}^{235})}{\epsilon}=\frac{\sum_n nA_n(\mathrm{U}^{235})}{\sum_n nA_n(\mathrm{Cf}^{252})}\cdot\bar{\nu}(\mathrm{Cf}^{252}).$$

III. RESULTS

A. Standard

The standard for all $\bar{\nu}$ values reported here is prompt $\bar{\nu}$ for spontaneous fission of Cf^{252}. An attempt has been made to obtain a best value of this quantity from data available at the present time.

Crane *et al.*[12,13] have given an absolute value of 3.53 ± 0.15; this was measured using a $MnSo_4$ bath calibrated by means of a mock-fission source and the National Bureau of Standards Ra–Be source. The same laboratory[14] has quoted a value of 3.8 ± 0.16. It is not clear whether this figure is a revision of the earlier measurement due to error in the standard source or whether it was obtained independently using a large liquid scintillation counter. In view of this uncertainty neither of these values has been included in our analysis.

Relative measurements of Cf^{252} spontaneous $\bar{\nu}$ have been reported by Hicks *et al.*,[15] Diven *et al.*,[16] and Meadows and Whalen,[17] the values being based directly or indirectly on thermal $\bar{\nu}$ for U^{235}.

Since 1960, several independent absolute determinations have been made and the over-all measure of agreement between these is extremely good.[18,19] The relevant details are summarized in Table II.

The assessment of the best value has been based on the most recent values available from each laboratory although some of these are still unpublished and complete experimental details are not available at the present time. The Stockholm and Los Alamos measurements employed very similar techniques and may have common systematic errors. We have therefore taken the unweighted mean of the two most recent values and assigned an error of ±0.03. The over-all weighted mean then becomes 3.782 ± 0.024. This is not expected to change very much when the unpublished values are finalized and it has therefore been taken as the standard for the $\bar{\nu}$ measurements in this paper.

Relative values of $\bar{\nu}$ do not include the error in this standard; for absolute values the error on the standard is compounded in the usual way with the experimental error on the ratio $\Sigma nA_n(\mathrm{U}^{235})/\Sigma nA_n(\mathrm{Cf}^{252})$.

B. Corrections and Errors

The $\bar{\nu}$ values obtained after the data processing described in Sec. II H may deviate from the true values for a number of reasons. These are dealt with under the following headings: (1) Statistical limitations; (2) Changes of counter efficiency; (3) Fission-spectra differences; (4) Fissions by neutrons degraded in energy; (5) Impurities in the fissile deposit; (6) Inaccuracy of fission-chamber positioning; (7) Preferential detection of certain fission events; (8) Anisotropy of fission-neutron emission; (9) Additional fissions occurring during the gate; (10) False gates; (11) Uncertainties in the mean primary energy; (12) Data processing errors; (13) Experimental limitations.

Comparison of U^{235} with Cf^{252} introduces the errors and corrections listed under Secs. III B3, 7–8; their magnitude changes with the energy of the neutrons incident on the U^{235} nucleus.

In Sec. II B6, the possible error arises through the difference in physical construction of the Cf^{252} and U^{235} fission chambers.

1. Statistical Limitations

It can be shown that the statistical error on the number of neutrons per fission is slightly less than that based on the reciprocal of the square root of the total number of detected counts; the error is given by

$$\left[\sum_{i=0}^{i\,\max} i^2 g_i-\left(\sum_{i=0}^{i\,\max} ig_i\right)^2\left(\sum_{i=0}^{i\,\max} g_i\right)^{-1}\right]^{-1/2}\left[\sum_{i=0}^{i\,\max} g_i\right]^{-1},$$

[12] W. W. T. Crane, G. H. Higgins, and S. G. Thompson, Phys. Rev. **97**, 242, 1727 (1955).
[13] W. W. T. Crane, G. H. Higgins, and H. R. Bowman, Phys. Rev. **101**, 1804 (1956).
[14] H. R. Bowman and S. G. Thompson, Proc. UN Intern. Conf. Peaceful Uses At. Energy, 2nd, Geneva **15**, 212 (1958).
[15] D. A. Hicks, J. Ise, and R. V. Pyle, Phys. Rev. **101**, 1016 (1956).
[16] B. C. Diven, H. C. Martin, R. F. Taschek, and J. Terrell, Phys. Rev. **101**, 1012, (1956).
[17] J. W. Meadows and J. F. Whalen, Phys. Rev. **126**, 197 (1962).
[18] I. Asplund, H. Condé, and N. Starfelt, Försvarets Forskningsanstalt Avdelning (Stockholm) 4 Rapport A 4200–411, 1961 (unpublished).
[19] I. Asplund-Nilsson, H. Condé, and N. Starfelt, Nucl. Sci. Eng. **16**, 124 (1963).

TABLE II. Post-1960 measurements of prompt $\bar{\nu}$ for Cf^{252} spontaneous fission.

Laboratory	Method	Investigators and date	Prompt $\bar{\nu}$
Stockholm	Neutron-proton scattering in an anthracene crystal at the center of a large liquid scintillation counter	Asplund, Condé, and Starfelt (1961)[a]	3.78 ±0.04
		Asplund, Condé, and Starfelt [unpublished, quoted in Asplund-Nilsson (1963)[b]]	3.82 ±0.04
		Asplund-Nilsson, Condé, and Starfelt (1963)[c]	3.799±0.034
Los Alamos	Neutron-proton scattering in hydrogen-filled proportional counter at center of large liquid scintillation counter	Diven and Hopkins. Preliminary value (1962)[d]	3.73 ±0.12
		Diven and Hopkins (private communication) (1963)	3.771±0.030
AERE Harwell	Photodisintegration of deuteron in a gridded ionization chamber at center of Harwell "Boron-pile"	Colvin and Sowerby (private communication) (1963)	3.780±0.053
AWRE Aldermaston	Neutron output of Cf sample measured by waxcastle comparison with Harwell Pu^{240} standard source. Fission rate separately determined	Moat, Mather, and McTaggart (1961).[e] Value corrected for fission neutron spectral differences of Cf^{252} and Pu^{240}	3.77 ±0.07

[a] See Ref. 18. [b] See Ref. 3. [c] See Ref. 19. [d] See Ref. 5. [e] See Ref. 7.

where g_i is the number of gates for which i neutrons are detected. All the statistical errors for the $\bar{\nu}$ results were computed on this basis.

2. *Changes of Counter Efficiency*

The calculated statistical error on the determination of counter efficiency using the Cf^{252} chamber was 0.18% for a 10-min run. Analysis of 22 calibration runs performed over a period of three weeks yielded a root-mean-square deviation of 0.22%. This check demonstrates that drifts of efficiency with temperature and other causes were negligibly small.

3. *Fission-Spectra Differences*

Since the U^{235} fission neutron spectrum may vary with the energy of the inducing neutrons and be different from that of the Cf^{252} used for efficiency calibration, there may be errors in the $\bar{\nu}$ values caused by the change of counter efficiency with detected neutron energy. No measurements have been made of the energy response of the counter but it has been calculated using a Monte Carlo computer program; the results are shown in Table III.

TABLE III. Monte Carlo calculations of efficiency for neutron detection by 76-cm-diam counter with 0.5% Gd loading.

Neutron energy (MeV)	0.1	0.5	1.5	3.0	14.0
Efficiency (%)	95	94	91	89	58

Terrell[20,21] has used evaporation theory and available experimental data to derive an expression for the variation of mean energy of fission neutrons, $\bar{E}$, with $\bar{\nu}$ for any nuclide: the expression is $\bar{E}=0.74+0.653(\bar{\nu}+1)^{1/2}$ MeV. This relationship, however, does not allow for the evaporation of neutrons prior to fission which occurs at high energies (see Sec. IV). At 8-MeV incident-neutron energy, for example, the excitation is sufficient for the evaporation of a neutron with an energy of about 1 MeV followed by fission of U^{235} compound nucleus. The mean energy of all the emitted neutrons may thus be even lower than that in the case of thermal fission. Because of the lack of experimental evidence on this point we have made use of Terrell's expression. We have also used his assessment of the best mean experimental values for $\bar{E}$ given in his paper (see Ref. 21). These are 2.15 MeV for Cf^{252} and 1.95 MeV for thermal-neutron-induced fission of U^{235}. In addition, our calculations assumed a Maxwellian distribution of emitted-neutron energies and the Monte Carlo results for the energy response of the counter (Table III). The outcome of these calculations is that an uncorrected thermal-$\bar{\nu}$ value would be too high by 0.225% and the 8.0-MeV value too high by 0.03%. The $\bar{\nu}$ values were corrected on the basis of the above computation, the correction being a reduction in $\bar{\nu}$ of 1.13% per MeV difference between the calculated $\bar{E}$ values for U^{235} and the value of $\bar{E}$ for Cf^{252}.

4. *Fissions by Neutrons Degraded in Energy*

The combined $\bar{\nu}$ and fission-time sorting arrangement shown in Fig. 5 became available towards the end of the experiment. Prior to this, fission-time spectra were only obtained at selected energies because of the long running times required. Table IV shows the "thermal" contributions to the fission rate and the corrections applied to the $\bar{\nu}$ values.

Both pulsed and dc beams were employed for the 3 MeV work; after full correction the dc $\bar{\nu}$ value was 2.753±0.024 and the TOF value 2.749±0.023. The good agreement of these two values suggests that the corrections applied were reasonable.

In all measurements the time resolution of the $\bar{\nu}$ TOF selection arrangement was sufficient to eliminate all secondary neutron groups revealed by the TOF spectra. However, any neutron groups produced by target impurities, backing, surface films, etc. with energies very close to that from the $d-d$ reaction could cause

[20] J. Terrell, Phys. Rev. **113**, 527 (1959).
[21] J. Terrell, Phys. Rev. **127**, 880 (1962).

TABLE IV. Corrections to $\bar{\nu}$ for "thermal" neutrons.

Neutron energy MeV	"Thermal" contribution[a] to the fission rate (%) Measured	Assumed	Correction to $\bar{\nu}$ (%)
0.25	···	8.5±4	0.24±0.11
0.35	···	8.5±4	0.20±0.09
0.5	···	8.5±4	0.19±0.09
0.75	16 ±3.5	8.5±4	0.13±0.06
0.85	···	8.5±4	0.36±0.17
1.0	5.8±1.8	8.5±4	0.27±0.13
1.25	···	8.5±4	0.46±0.22
1.5	···	8.5±4	0.54±0.25
2.0	···	8.5±4	0.76±0.36
2.5	8.2±3.1	8.5±4	0.85±0.40
3.0	···	8.5±4	{0.09±0.04 {1.04±0.49
4.0	8.8±1.7	8.8±1.7	1.55±0.30
5.0	···	16.0±8	0.31±0.15
6.0	19.4±4.4	19.4±4.4	0.45±0.10
7.0	···	22.0±4	0.61±0.11
8.0	25.0±2.7	25.0±2.7	0.76±0.09

[a] The values given are expressed for dc conditions; for pulsed measurements these figures must be reduced by the ratio of fourfold resolving time to beam-pulse separation. The measured values were used to derive an assumed variation of contamination with energy.

trouble. No such groups were revealed by TOF spectra taken with blank targets. With deuterium targets no broadening of the primary-energy peak relative to the γ-ray peak was observed using time resolutions between 4.5 and 6.5 nsec. There remains the possibility that some neutrons slightly degraded in energy by the collimator were contained in the main peak.

An attempt has been made to calculate the effect of the collimator using the Monte Carlo method and the AWRE STRETCH computer. The program was already in existence and not ideally suited to this particular application. However, using this program it was possible to establish for an 8-MeV source that less than 1% of the neutrons reaching the fission chamber came from scatter in the collimator; these were in the energy group 6–8 MeV. In order to improve statistics on the score of secondary particles reaching the fission chamber, the source neutrons were assumed to be emitted in a narrow forward cone such that about half of these reached the chamber directly. The cone had an opening angle sufficient to see most of the polyethylene and mild steel collimator plugs (as described by Moat *et al.*[7]), but not the main body of the shielding. The transmission of this was sufficiently low to ensure that very few of the neutrons outside the selected cone could reach the fission chamber.

5. *Impurities in the Fissile Deposit*

Analysis by mass spectroscopy showed that the coating of the uranium foils consisted of 92.89% U^{235}, 5.69% U^{238}, 1.20% U^{234}, and 0.22% U^{236}. Thus it is necessary to consider the error caused by fissions in these materials. Experimental $\bar{\nu}$ values available for U^{238} at 1.25 MeV and above suggest that the variation of $\bar{\nu}$ with incident neutron energy E is given by $\bar{\nu}\,(U^{238}, E)=2.33+0.15\,E$.[22]

No experimental results are available for U^{234} above 4 MeV so the following expression has been adopted[23]:

$$\bar{\nu}(U^{234}, E)=2.33+0.125\,E.$$

This is derived from the calculations of Bondarenko *et al.*[24] on the variation of $\bar{\nu}$ with A and Z, together with the mass tables of Everling *et al.*[25] and the assumption $d\bar{\nu}/dE=0.125$.

Using $\bar{\nu}$ values for U^{238} and U^{234} from the above expressions along with appropriate fission cross sections from BNL 325, the corrections to the U^{235} measurements have been calculated. The greatest correction is +0.18% at 8 MeV, while at 5 MeV and below the error is negligible. The quoted $\bar{\nu}$ values and ratios given in the table of final results (Table VI) have been adjusted accordingly.

6. *Inaccuracy of Fission-Chamber Positioning*

The fission chambers were located inside the axial tube of the scintillation counter by a stop so that their centers were at the middle of the sphere within ±0.1 cm. However, the Cf^{252} chamber had only one plate while the U^{235} chamber had sixteen plates spread over 5 cm of the axis. If the counter efficiency varied for neutrons originating at positions off center an error would result in the $\bar{\nu}$ measurements for U^{235}. Measurements of efficiency were carried out for displacements of the Cf^{252} chamber along the axis of the counter up to 10 cm from the center. The measured points indicate that the efficiency is constant to within 0.04% out to 3 cm. The most pessimistic estimate of the error due to using the distributed source is −0.1%. This effect is regarded as negligible.

7. *Preferential Detection of Certain Fission Events*

Since a discriminator bias has to be applied to the pulses from the fission chamber, fission pulses of small amplitude are excluded and the measured $\bar{\nu}$ value may therefore differ from a value averaged over all fission events. The fission-pulse amplitude is a function of the kinetic energies of the fragment pair, the angle of the fragments relative to the incident neutron, their energy loss in the fissile deposit, and the particular fragment which enters the counter gas. Since the neutron emission is known to be a function of the fission mode and may depend also on the fragment angle relative to the incident neutron (see also Sec. II B13), some error will be caused by the application of a bias to the fission

[22] K. Parker (private communication).

[23] This expression is in fair agreement with recent measurements up to 4 MeV by the present authors.

[24] I. I. Bondarenko, B. D. Kuzminov, L. S. Kutsayeva, L. I. Prokhorova and G. N. Smirenkin, Proc. UN Intern. Conf. Peaceful Uses At. Energy, 2nd, Geneva **15**, 353 (1958).

[25] F. Everling, L. A. Konig, J. H. E. Mattauch, and A. H. Wapstra, Nucl. Phys. **18**, 529 (1960).

pulses. Measurements have been made of the apparent $\bar{\nu}$ for Cf^{252} as a function of discriminator bias and are shown in Table V.

TABLE V. Variation of the apparent $\bar{\nu}$ of Cf^{252} with fission chamber bias.

Fission bias (fraction of maximum fission pulse height)	Fall in apparent $\bar{\nu}$ (from extrapolated zero bias value) (%)
0.2	0.08
0.4	0.26
0.6	0.80
0.8	2.15

The apparent $\bar{\nu}$ can be seen to fall off slowly at first and then more rapidly. This result is probably a consequence of the relationship between fragment kinetic energy and $\bar{\nu}$, but since the chamber is not gridded and the plate separation is less than the fragment range, the results cannot be interpreted simply. For calibration experiments, the Cf chamber was used with a bias of approximately 0.14 of the maximum fission-pulse amplitude thus giving a negligible error.

In the case of the U^{235} chamber a similar experimental determination is not possible because of the low fission rate; the magnitude of the effect may also change with incident neutron energy. Furthermore, in order to prevent the buildup of α pulses from the U^{235}, it is necessary to use a higher discriminator bias ($\sim$0.3 of maximum pulse height) than for Cf^{252}.

To allow for some uncertainty of the effect of using a higher bias on the U^{235} fission pulses, we include an error of $\pm 0.3\%$.

8. *Anisotropy of Fission Neutron Emission*

Neutrons from the fission fragments are generally assumed to be emitted isotropically in the fragment frame of reference and in the laboratory system the consequent peaking of the neutron distribution in the fragment direction has been well studied.[26,27] The scintillation counter efficiency is not independent of neutron direction because of the tube passing through its diameter, and hence the measured $\bar{\nu}$ for fission fragments traveling along the axis of the tube will be less than the $\bar{\nu}$ measured for other fragment directions. In the case of spontaneous fission, the fragments are emitted isotropically and therefore the hole through the counter has no effect on the measurement of $\bar{\nu}$. However, for neutron-induced fission, the angular distribution of the fission fragments is related to the direction of the incident neutron and has a maximum in this direction. The degree of anisotropy depends on the incident-neutron energy so that an error is caused in $\bar{\nu}$ measurements for induced fission, the magnitude of the error varying with incident energy. This error is interrelated with that of the previous Sec. III B7; but for clarity it is assumed here that there is no preferential detection of fission events.

An estimate of the magnitude of the error has been obtained by making some simplifications. The "hole" through which neutrons are lost has an effective radius larger than the physical radius of the tube because neutrons which pass through only short lengths of scintillator have a high chance of escape. This effective radius was rather crudely measured by obtaining the efficiency of the counter when the axial tube was filled with Cd-loaded polythene and comparing this with the normal efficiency. The change in efficiency was 1.3%, this corresponds to a loss-cone angle of 20° compared with the physical-cone angle of 10°. Taking the 20° angle, the data of Simmons and Henkel[28] for the fission-fragment anisotropy with 7.5 MeV incident-neutron energy, and the neutron angular distributions of Ramanna and Rama Rao,[27] the error produced in a 7.5-MeV-induced $\bar{\nu}$ measurement is 0.2% referred to the Cf^{252} calibration. Since the fragment anisotropy in the range thermal to 8 MeV is shown by Simmons and Henkel[28] to be a maximum at 7.5 MeV, the error due to this effect in any of the $\bar{\nu}$ measurements below 7 MeV is negligible. A correction of $+0.2\%$ has been made to the 7- and 8-MeV values.

9. *Additional Fissions Occurring During the Gate*

The electronics block diagram of Fig. 5 shows a unit labeled "double-fission detector," the purpose of which was to veto the output signal from the multiple-event analyzer to the pulse-height analyzer display whenever a second fission pulse occurred during the time the gate was open. Unless this was done, the prompt and capture pulses from the second fission would add to the number of counts but not to the number of gates and thus give an increased $\bar{\nu}$ value. The double-fission detector did not respond during the first 2 μsec of the 40 μsec gate and, in addition, did not eliminate double-fission events in which one of the fissions produced a small fission-chamber pulse and was undetected. However, these imperfections caused negligible errors and even in the case of Cf^{252} where the gating rate was about 3×10^5/h the error introduced was only about 0.05%.

10. *False Gates*

Occasionally the buildup of α-particle pulses from the U^{235} is sufficient to exceed the bias level in the fission circuit and a random coincidence between one of these buildup pulses and a scintillation-counter pulse will open the gate. The number of these false gates can be calculated from the measured resolving time of the slow coincidence unit, the scintillator pulse rate and the α buildup rate; the latter is given approximately by the

[26] J. S. Fraser, Phys. Rev. **88**, 536 (1952).
[27] R. Ramanna and P. N. Rama Rao, Proc. UN Intern. Conf. Peaceful Uses At. Energy, 2nd, Geneva **15**, 361 (1958).
[28] J. E. Simmons and R. L. Henkel, Phys. Rev. **120**, 198 (1960).

difference between the total number of gates and the reading of a scaler following the fission-chamber discriminator. This discriminator had to be set as low as practicable so that few fission events were excluded and, because of the steep rise of the α buildup rate at low bias settings, the number of false gates was occasionally larger than intended. The corrections for false gates were less than 0.25% except at 0.25, 0.35, and 1 MeV where the corrections were 0.52, 0.76, and 0.62%, respectively.

11. Uncertainties in the Mean-Primary Energy

Errors in the quoted values of incident energy are mainly due to the uncertainties in the thickness of the target and in the rate of energy loss of the bombarding particles. Selection of the correct bombarding-particle energy was achieved using proton-resonance equipment with the analyzing magnet; the $Li^7(p,n)$ threshold was used to calibrate this. The uncertainty in the mean energy was always less than 40 keV and the uncertainty in the spread about 10%.

12. Data Processing Errors

Since the coefficients of the correction matrix are obtained by a sampling process (Sec. II H), they are subject to statistical errors. In the simulation process 10 000 trials were made for each combination of genuine and background counts. In order to assess how the errors on the coefficients affected the corrected values of $\bar{\nu}$, several computer runs were carried out for Cf^{252} with each coefficient altered by plus or minus one standard deviation, the positive or negative sign being randomly chosen each time a coefficient was required. These checks indicated that no significant error was introduced by inaccuracies in the coefficients.

To test the working of the background subtraction and dead-time correction program, a series of efficiency runs using Cf^{252} were undertaken in the presence of accelerator-produced backgrounds of different intensities. All the results, after correction, were in good agreement for backgrounds up to 0.6 counts/gate, which was the maximum level tolerated in any $\bar{\nu}$ run (Sec. II E).

Variations of the background level during the course of an experiment may be another possible source of error since only the mean rate is used in the correction procedure. The background rare was monitored by a pen recorder and runs with variations greater than $\pm 10\%$ were rejected. By combining the observed multiplicity distributions of two efficiency runs of different background (of the kind described above) it is possible to get the composite multiplicity distribution which would be obtained in a run where the background alternated between the two levels. The usual correction procedure then gives a "composite efficiency." Experimental runs with appropriate background levels were recorded, so that a series of composite efficiencies could be derived which had the same mean background but different maximum and minimum levels. Over the range of tolerated mean backgrounds, the permitted variations caused no significant changes in the efficiency.

13. Experimental Limitations

An experimental limitation occurs in the present work because the fissile foils were set normal to the incident neutron beam. The fragments trapped in the fissile deposit (about 5%) are those moving close to 90° to the incident neutron direction; consequently, errors may exist if there is a sharp correlation of ν with fragment angle. Further work is necessary to clear this point. A second limitation to be considered is the possible detection of some short-period γ rays during the 40 μsec gating interval. Maienschein *et al.*[29] give some data on such γ rays following thermal fission of U^{235}. We deduce from these measurements that the contribution of these γ rays to the mean count per fission is small; the effect on $\bar{\nu}$ depends on the difference between the contributions for Cf^{252} and for U^{235} at each incident neutron energy. We therefore cannot rule out the possibility of significant effects at energies other than thermal, the only energy for which data on these γ rays exist.

C. $\bar{\nu}$ Values

Values of $\bar{\nu}$ obtained after making all corrections considered in Sec. III B are tabulated in Table VI. This table also lists the spreads in incident-neutron energy due to the target thickness and the total correction applied to the $\bar{\nu}$ data. Errors are quoted for both relative and absolute $\bar{\nu}$ values as explained in Sec. III A, and for convenience the final column of Table VI gives the ratio $\bar{\nu}(E):\bar{\nu}$ (thermal).

The fitting of the data with polynomial expressions was carried out with a least-squares computer program which included chi-squared tests. A single straight line could not be fitted over the entire energy range. The best single curve fit was the quadratic

$$\bar{\nu}(E)=(2.423\pm0.008)+(0.088\pm0.008)E + (0.0088\pm0.0011)E^2,$$

which had a 30% probability and is the curve drawn on the plot of the results in Fig. 6.

Linear fits starting at the lowest and highest energies and gradually including more and more points were also tried. Very good fits were obtained for the ranges 0–3 and 3–8 MeV. These were:

$$\bar{\nu}(E)=(2.418\pm0.008)+(0.109\pm0.006)E \quad \text{from 0 to 3 MeV},$$

and

$$\bar{\nu}(E)=2.200\pm0.023)+(0.181\pm0.005)E \quad \text{from 3 to 8 MeV}.$$

[29] F. C. Maienschein, R. W. Peelle, W. Zobel, and T. A. Love, Proc. UN Intern. Conf. Peaceful Uses At. Energy, 2nd Geneva **15**, 366 (1958).

TABLE VI. U^{235} prompt $\bar{\nu}$ values.

Mean incident neutron energy E (MeV)	Neutron energy spread due to target thickness (keV)	Total correction applied to $\bar{\nu}$ (%)	[a] $\bar{\nu}$	[b] Error for relative values	[c] Error for absolute values	[d] $\bar{\nu}$ (E) / $\bar{\nu}$ (thermal)
Thermal	...	−0.225	2.412	0.012	0.020	1.000
0.040	...	−0.01	2.420	0.014	0.021	1.000±0.008
0.14	40	−0.25	2.423	0.042	0.045	1.001±0.023
0.23	25	+0.52	2.490	0.022	0.027	1.028±0.010
0.33	115	+0.72	2.478	0.021	0.026	1.023±0.010
0.43	115	+0.00	2.475	0.020	0.025	1.023±0.010
0.70	145	+0.11	2.457	0.016	0.022	1.015±0.008
0.84	70	+0.22	2.529	0.021	0.026	1.044±0.010
0.93	190	+0.63	2.499	0.020	0.026	1.032±0.010
1.17	175	+0.38	2.557	0.021	0.027	1.056±0.010
1.47	130	+0.47	2.583	0.020	0.026	1.067±0.010
1.94	135	+0.71	2.656	0.021	0.027	1.097±0.010
2.44	120	+0.72	2.689	0.022	0.028	1.111±0.011
2.96	110	[e] +1.34 dc	2.751	0.016	0.024	1.135±0.009
3.87	580	+1.40	2.933	0.022	0.029	1.211±0.011
4.91	385	+0.25	3.074	0.027	0.033	1.270±0.013
5.94	270	+0.51	3.273	0.025	0.033	1.352±0.012
6.96	210	+0.95	3.490	0.027	0.035	1.442±0.013
7.96	205	+1.04	3.666	0.037	0.044	1.509±0.017

[a] These values are based on $\bar{\nu}$ (Cf^{252} spont.) $=3.782\pm0.024$.
[b] This error does not include the error in $\bar{\nu}$ (Cf^{252}, spont.).
[c] Includes error in $\bar{\nu}$ (Cf^{252}, spont.).
[d] The error includes that of the thermal value.
[e] The 2.96 MeV $\bar{\nu}$ value is comprised of dc and TOF measurements; the resultant of all corrections to the TOF value is −0.01.

The first had a probability of 20% and the second a probability of 60%.

The compilation of post-1960 results given in Table VII allows comparison to be made with values obtained elsewhere. Accuracies of better than 1% for relative measurements have been achieved in the most recent measurements and amongst these there seems to be a fair measure of agreement on the slope $d\bar{\nu}/dE$ at low incident-neutron energies. Meadows and Whalen[17] give a value of 0.097 ± 0.008 MeV^{-1}, while Diven and Hopkins[5] get 0.122 ± 0.008 MeV^{-1}.

The quadratic and straight-line fits of the present paper will not satisfy the 14 MeV results in Table VII. Extrapolation of the quadratic gives a 14-MeV value of 5.36- and the 3–8-MeV line continued would give 4.82. There must therefore be some flattening off in the curve of $\bar{\nu}$ against E at higher energies than 8 MeV. It is possible that the 14-MeV $\bar{\nu}$ results have been depressed by unsuspected thermal and low-energy-induced fissions although it is doubtful if this could account for all the discrepancy. A preliminary value for $\bar{\nu}$ at 12.3 MeV, obtained here using the TOF selection system, is 4.48

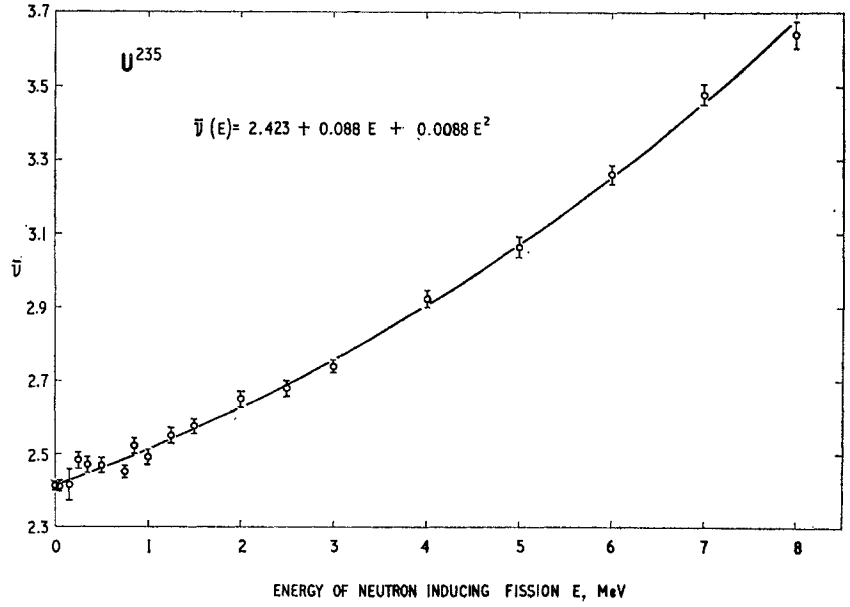

FIG. 6. Prompt $\bar{\nu}$ for U^{235} as a function of incident-neutron energy. The curve drawn is the quadratic fit given.

TABLE VII. Post-1960 measurements of prompt $\bar{\nu}$ for U^{235} induced fission.

Mean incident neutron energy E (MeV)	Prompt $\bar{\nu}$	Error for[a] relative values	Error for[b] absolute values	$\bar{\nu}(E)$[c] / $\bar{\nu}$ (thermal)	$\bar{\nu}$ normalized to $\bar{\nu}$ (Cf^{252} spont.) = 3.782[d]	Investigators and method
Standard—$\bar{\nu}$ (Cf^{252} spont.) = 3.771±0.030. measured						Diven and Hopkins (private communication).
Thermal (measured)	2.425	0.020	0.028	1.000	2.432	
0.280±0.090	2.438	0.022	0.029	1.005±0.012	2.445	Loaded liquid scintillation counter, $\epsilon\sim80\%$.
0.470±0.080	2.456	0.022	0.030	1.013±0.012	2.463	Neutron pulses gated (~60 μsec) by fission-chamber pulse.
0.815±0.060	2.471	0.026	0.033	1.019±0.014	2.478	
1.08 ±0.05	2.530	0.026	0.033	1.043±0.013	2.537	
3.93 ±0.29	2.937	0.030	0.038	1.211±0.016	2.946	
14.5 ±1.0	4.626	0.075	0.084	1.908±0.035	4.639	
Standard—$\bar{\nu}$ (U^{235} thermal) = 2.414±0.030. BNL 325 av used to determine substandard $\bar{\nu}$ (Cf^{252} spont.) = 3.754±0.048						Meadows and Whalen (Ref. 17).
Thermal (assumed)					2.432	
0.03	2.421	0.025	0.039	1.002±0.010	2.439	Energy errors estimated from graph in ANL 6399 (1961).
0.20 ±0.03	2.436	0.016	0.034	1.009±0.007	2.454	
0.62 ±0.05	2.470	0.019	0.036	1.023±0.008	2.488	Polyethylene and paraffin containing 10 BF_3 detectors, $\epsilon\sim5\%$.
1.11 ±0.04	2.520	0.018	0.036	1.044±0.008	2.539	
1.58 ±0.03	2.580	0.020	0.037	1.069±0.008	2.599	Neutron pulses gated (~800 μsec) by fission chamber pulse.
1.76	2.575	0.021	0.039	1.067±0.009	2.594	
Standard—$\bar{\nu}$ (Cf^{252} spont.) = 3.77±0.07. measured[e]						Moat, Mather and McTaggart (Ref. 7).
0.075±0.020	2.44 (2.39)	0.030	0.050	1.008[f]	2.448	Loaded-liquid scintillation counter (cylindrical model), $\epsilon\sim65\%$.
2.50 ±0.11	2.66 (2.60)	0.060	0.090	1.095±0.028	2.668	Neutron pulses gated (~23 μsec) by fission-chamber pulse.
14.20 ±0.18	4.37[g] (4.28)	0.023	0.090	1.798±0.024	4.384	
Standard—(Cf^{252} spont.) = 3.782±0.024. weighted av						D. S. Mather, P. Fieldhouse, and A. Moat.
12.3	4.48	0.054	0.061	1.852±0.024	4.48	Preliminary value using time-of-flight energy selection. Loaded-liquid scintillation counter (spherical model) as for present paper, $\epsilon\sim85\%$. Neutron pulses gated (~40 μsec) by fission-chamber pulse.
Standard—Absolute efficiency from photodisintegration of deuteron						Sowerby (private communication).
Thermal	2.414		0.030		2.415	"Boron-pile"—graphite containing $^{10}BF_3$ detectors, $\epsilon\sim60\%$. Neutron pulses gated (~4 msec) by fission-chamber pulse.

[a] This error does not include the error in the standard.
[b] Includes the error in the standard.
[c] This error includes the relative error on the thermal value.
[d] 3.782 is the weighted mean of selected data for $\bar{\nu}$ (Cf^{252}, spont.) as discussed in Sec. III A.
[e] The value reported originally was 3.69±0.07. We have now applied the spectral correction of +2.1% described in the "note added in proof" to the original paper. The figures in brackets are those initially reported.
[f] These ratios are based on $\bar{\nu}$ (U^{235} thermal) = 2.43±0.05 calculated from the 75-keV value.
[g] This measurement was made using a dc beam and therefore may be subject to some "thermal" contamination.

which is not fitted by the quadratic (4.72) but does lie on the straight line (4.41). An extension of the present measurements to include several points in the 8–14 MeV range is desirable in order to clarify the position.

IV. DISCUSSION

Estimates can be made of the variation of $\bar{\nu}$ with the energy of the incident neutrons by assuming that the fission neutrons are all evaporated from the fission fragments and that all the energy of the incident neutrons appears as additional excitation of the fragments. It is assumed that the fragments lose their excitation as the binding energy and kinetic energy of the evaporated neutrons. Residual excitation of the fragments will then be dissipated by the emission of γ quanta. This simple picture predicts a linear function for $\bar{\nu}$ with $d\bar{\nu}/dE$ equal to about 0.13 MeV^{-1}—in good agreement with the value deduced from thermal and 14-MeV $\bar{\nu}$ measurements on U^{235}. More refined approaches to the prediction of $d\bar{\nu}/dE$ have been discussed previously.[24,30,31]

The simple approach to prediction of $d\bar{\nu}/dE$ can be expected to apply only for incident neutron energies below the $(n,n'f)$ threshold. Above this threshold some neutron scatter events occur which leave the residual (U^{235}) nucleus with an excitation above its fission barrier so that fission of this nucleus takes place. The $(n,n'f)$ process cannot be distinguished experimentally

[30] R. B. Leachman, Los Alamos Research Report, 1863, 1954 (unpublished).
[31] R. B. Leachman, Phys. Rev. **101**, 1005 (1956).

from simple fission so that any fission measurements above about 6 MeV include effects due to $(n,n'f)$. The fission cross section, for example, shows a marked increase at the $(n,n'f)$ threshold. We are interested here in any changes which might occur in $\bar{\nu}$ at this threshold. The effect of the $(n,n'f)$ process on $\bar{\nu}$ has been discussed by Leachman[30] and more recently by Vasil'ev *et al.*[32] It can be shown that, in general, there will be a step in the $\bar{\nu}$ function of magnitude

$$\Delta\bar{\nu}=\frac{\sigma(n,n'f)}{\sigma(n,f)+\sigma(n,n'f)}[1-\bar{\nu}_1+\bar{\nu}_2], \quad (1)$$

where $\sigma(n,n'f)$ and $\sigma(n,f)$ are the cross sections at energy E, E is the incident neutron energy at which the step magnitude is to be evaluated; $\bar{\nu}_1$ is the $\bar{\nu}$ for fission of the U^{236} compound nucleus at excitation $(E+E_b)$, i.e., fission of U^{235} by neutrons of energy E without prior evaporation of a neutron; $\bar{\nu}_2$ is the $\bar{\nu}$ for fission of the U^{235} compound nucleus at excitation $(E-2T)$, equivalent to fission of U^{234} by neutrons of energy $(E-2T-E_b')$; E_b is the binding energy of the last neutron in the U^{236} nucleus; E_b' is the binding energy of the last neutron in the U^{235} nucleus; and T is the characteristic nuclear temperature for the evaporation of neutrons.

Above the $(n,n'f)$ threshold, the measured neutron emission, $\bar{\nu}_3$, is given by

$$\bar{\nu}_3=\bar{\nu}_1+\Delta\bar{\nu}. \quad (2)$$

Using (2), Eq. (1) can be rewritten as

$$\Delta\bar{\nu}=\frac{\sigma(n,n'f)}{\sigma(n,f)}[1+\bar{\nu}_2-\bar{\nu}_3]. \quad (3)$$

We now evaluate $\Delta\bar{\nu}$ and $\bar{\nu}_1$ using Eqs. (3) and (2), and the following numerical values: $\bar{\nu}_2=2.63$ (based on our own preliminary $\bar{\nu}$ measurements of U^{234} from 1 to 4 MeV); $\bar{\nu}_3=3.666$ (8-MeV value from present paper); $\sigma(n,f)=1.20$ b, and $\sigma(n,n'f)=0.60$ b both from Hughes and Schwartz[33]; $E_b=6.4$ MeV, and $E_b'=5.2$ MeV, both from Everling *et al.*[25]; and $T=0.37$ MeV Vasil'ev *et al.*[32] We find $\Delta\bar{\nu}=-0.02$ and $\bar{\nu}_1=3.69$. Evaluation is carried out at 8 MeV since any step in $\bar{\nu}$ is expected to be smoothed due to the effects of energy spread of evaporated neutrons and the changing probability of fission of the residual nucleus. The small magnitude of $\Delta\bar{\nu}$ indicates that no step should be apparent in the $\bar{\nu}$ curve.

An interesting feature of the results presented in this paper is that the slope of the $\bar{\nu}$ function increases from a value which is less than to a value which is greater than that expected (0.13 MeV^{-1}) on the simple picture mentioned earlier. The value of $\bar{\nu}_1$ calculated above is of interest because it implies that the high value of $d\bar{\nu}/dE$ for simple fission, observed just below the $(n,n'f)$ threshold, continues to apply up to at least 8 MeV. However, the energy range of major interest is thermal to 6 MeV because there is no ambiguity in the excitation at which fission takes place; it is this region which we consider here. Bondarenko *et al.*[24] have pointed out that there are two factors which are expected to lead to a *decreasing* slope; these are, (a) the increasing binding energy of successive neutrons evaporated from a fragment, and (b) the greater kinetic energy associated with neutrons evaporated from more highly excited fragments. It therefore appears that some over-riding mechanism is responsible for the observed increase in slope[34] and we will examine some possibilities.

In fission at high excitation, nuclei may tend to cross the saddle point via channels which are either unavailable or improbable at lower excitation. Some properties of fission well established for the thermally induced or spontaneous case may be modified considerably at higher energies. We consider three mechanisms which could account for a nonproportional increase of mean fission-fragment excitation with increasing incident-neutron energy. These are, (a) increasing preference for those mass ratios which carry the greatest excitation; (b) increase in the fragment excitation over all mass ratios at the expense of fragment kinetic energy; and (c) decrease in the energy carried off by photons, the balance being available for neutron emission.

After consideration of these mechanisms, we examine the question of whether the neutrons emitted in fission at high excitation [but below the $(n,n'f)$ threshold] do, in fact, all originate from the fragments, or whether some may be evaporated from the fissioning nucleus by a process distinct from $(n,n'f)$.

It is well known that the valley in the mass distribution from fission fills as the incident neutron energy is raised and it is natural to attempt to find some correlation between this effect and the neutron emission.[35] Gibson *et al.*[36] and Milton and Fraser[37] showed that for U^{235} thermal fission, a correlation exists between mass ratio and fragment kinetic energy. The kinetic energy was found to decrease sharply by approximately 40 MeV as symmetry was approached. Measurements of the neutron emission as a function of mass ratio by Apalin *et al.*[38] have now shown conclusively that this

[32] Yu. A. Vasil'ev, Yu. S. Zamyatnin, Yu. I. Il'in, E. I. Sirotinin, P. V. Toropov, and É. F. Fomushkin, Zh. Eksperim i Teor. Fiz. **38**, 671 (1960) [English transl.: Soviet Phys.—JETP **11**, 483 (1960)].

[33] D. J. Hughes and R. B. Schwartz, Brookhaven National Laboratory, Report No. 325, 1958 (unpublished).

[34] For this discussion we assume that the experimental limitations described in Sec. III B13 are not responsible for the observed change in slope of the $\bar{\nu}$ function.

[35] Terrell (Ref. 21) has suggested that part of the increase of $\bar{\nu}$ with excitation may be due to changes in the fission-product distribution.

[36] W. M. Gibson, T. D. Thomas, and G. L. Miller, Phys. Rev. Letters **7**, 65 (1961).

[37] J. C. D. Milton and J. S. Fraser, Phys. Rev. Letters **7**, 67 (1961).

[38] V. F. Apalin, Y. N. Gritsyuk, I. Y. Kutikov, V. I. Lebedev, and L. A. Mikaelyan, Nucl. Phys. **38**, 193 (1962).

decrease in fragment kinetic energy is matched by an increased neutron yield. Making allowance for the experimental dispersion in fragment mass, Apalin estimated that 6 neutrons are emitted in symmetric fission of U^{235}. In his recent study of the neutron yields from individual fission fragments, Terrell[21] demonstrates the applicability of a universal function $\nu_f(M)$, the number of neutrons emitted by a fragment of mass M. Terrell's universal function predicts close to 7 neutrons for symmetrical fission of U^{236} compound nucleus, in good agreement with the measurements of Apalin. In order to test whether this preferential neutron emission near symmetry could account for the observed increase in slope $d\bar{\nu}/dE$, the universal function $\nu_f(M)$ was folded in with thermal and also with 14-MeV fission mass distributions.[39] The 14-MeV neutron emission, $\langle\nu_f(M)\rangle_{\text{av}}$ was found to be greater by 0.13 than that for thermal fission. Subtracting this quantity from the 14-MeV $\bar{\nu}$ value to remove the effects of changes in the mass distribution, we find the average slope from thermal to 14 MeV is 0.13 MeV^{-1}. This is still substantially higher than the observed slope in the low-energy region and at 8 MeV it predicts a lower $\bar{\nu}$ than has been observed. It is clear that the effect accounts for only a small part of the observed nonlinearity.

The simple prediction of $d\bar{\nu}/dE$ mentioned at the beginning of this discussion contains a major assumption; that the entire kinetic energy of the incident neutron goes to increase the excitation of the two fragments, the total fragment kinetic energy remaining the same as for thermal fission. Recently Okolovich *et al.*[40] have measured the mean kinetic energy of fragments from thermal and 5 MeV fission of U^{235} ;they found that the energies were the same to $\pm 0.1\%$. A later paper[41] shows that for 15 MeV fission of U^{235}, the fragments have a kinetic energy lower by 1.5 ± 0.3 MeV than for thermal fission. It may be fortuitous that the kinetic energies agree closely at these three energies, for Okolovich *et al.* also report[40] that preliminary measurements in the energy range 0.3 to 1.5 MeV show appreciable changes in the kinetic energy. (It is interesting to note that the $\bar{\nu}$ values at 0, 5, and 14 MeV lie on a line with $d\bar{\nu}/dE=0.13$ MeV^{-1}.) With the present information it is not possible to say whether or not the observed changes in $d\bar{\nu}/dE$ are due to changes in the fragment kinetic energy.

The increase in $d\bar{\nu}/dE$ could occur at the expense of the energy carried off by the prompt fission γ rays. However, Leachman[42] has calculated that the γ energy should increase with increasing energy of the incident neutron, his figures being 3.8 MeV for thermal fission of U^{235}, and 4.5 MeV for 14-MeV fission. Actual measurements show that the energy for thermal fission is about 7.5 MeV.[29,43] Recently, Protopopov and Shiryaev[44] have found that there is no difference in the γ emission from thermal, 2.8- and 14.7-MeV neutron-induced fission of U^{235}. It appears that the increase in $d\bar{\nu}/dE$ does not occur at the expense of the γ-emission energy.

In the mechanisms considered so far, it has been assumed that below the $(n,n'f)$ threshold the fission neutrons are all emitted by the fragments; however, there is some experimental evidence that neutrons may be released by another process. Bowman *et al.*[45] have made measurements on the angular correlation between the fragments and neutrons from Cf^{252} spontaneous fission. They suggest that their results are consistent with some 10–20% of the neutrons leaving the fissioning nucleus before scission rather than being evaporated from the moving fragments. Unfortunately no similar experiments have been carried out for induced fission below the $(n,n'f)$ threshold and it is necessary to resort to work carried out at 14-MeV inducing energy and above. Vasil'ev *et al.*[32] have made measurements of the energy spectra of neutrons emitted in the 14-MeV induced fission of U^{235} and U^{238} and from each observed spectrum, have isolated an evaporation (or pre-fission) and a fragment component. They found that for U^{235} $(16\pm 2)\%$, and for U^{238} $(21\pm 2)\%$ of neutrons do not come from the fragments. These figures were compared with a calculated value of about 10% obtained on the assumption that the pre-fission evaporation neutrons all arise in $(n,n'f)$ reactions and that the cross section for this process can be obtained from the total-fission cross section by subtracting the value for the (n,f) cross section at the $(n,n'f)$ threshold. They conclude that the (n,f) cross section must in fact decrease above the $(n,n'f)$ threshold, but an alternative interpretation of their results is that the additional evaporation neutrons are produced after the saddle point but before scission. Measurements by Clarke[46] of the spectrum and yield of neutrons produced by 14-MeV neutrons incident on uranium have been interpreted by Hanna and Clarke[47] in terms of such a process. The results of Vasil'ev *et al.* and Clarke and Hanna imply the emission of 3.4 ± 0.3 and 2.1 ± 0.5 neutrons, respectively, from the fragments. It is interesting to note that the angular-correlation measurements of Harding and Farley[48] show that, even at the very high excitation energy obtained using 147-MeV protons on uranium, only about 2.5 ± 1 neutrons (out of a total emission of 13) appear to originate from

[39] S. Katcoff, Nucleonics **18**, No. 11, 201 (1960).
[40] V. N. Okolovich, G. N. Smirenkin, and I. I. Bondarenko, Soviet J. At. Energy (English transl.) **12**, 491 (1963).
[41] V. N. Okolovich and G. N. Smirenkin, Soviet J. At. Energy (English transl.) **13**, 652 (1963).
[42] R. B. Leachman, Los Alamos Research Report 1918, 1955 (unpublished).
[43] J. E. Francis and R. L. Gamble, Oak Ridge National Laboratory Report No. 1879, 1955, p. 20 (unpublished).
[44] A. N. Protopopov and B. M. Shiriaev, Zh. Eksperim. i Teor. Fiz. **34**, 331 (1958) [English transl.: Soviet Phys.—JETP **7**, 231 (1958)].
[45] H. R. Bowman, S. G. Thompson, J. C. D. Milton, and W. J. Swiatecki, Phys. Rev. **126**, 2120 (1962).
[46] R. L. Clarke, Can. J. Phys. **39**, 957 (1961).
[47] G. C. Hanna and R. L. Clarke, Can. J. Phys. **39**, 967 (1961).
[48] G. N. Harding and F. J. M. Farley, Proc. Phys. Soc. (London) **A69**, 853 (1956).

the fragments. (However, Marquez[49] has pointed out that their results are consistent with all the neutrons being evaporated from the fragments if the mean neutron energy is 6 MeV.)

The emission of neutrons after the saddle point appears to be an acceptable model; the neutrons would probably be evaporated from the neck portion of the fissioning nucleus. This portion, at a late stage in the fission process, may consist largely of neutrons surplus to the requirements of the massive end-portions which are condensing into normal individual nuclei. It is not clear how this picture could explain an increase in $d\bar{\nu}/dE$ with excitation but it does at least make feasible high values for that slope which we have so far been unable to explain in this discussion. The results of this paper show that the slope $d\bar{\nu}/dE$ over the region 3–8 MeV is 0.18 MeV^{-1}, which implies a binding energy per neutron of $(5.5-E_n)$ MeV, where the emitted neutron energy E_n is probably close to 1 MeV. Neutron binding energies as low as this might apply in the neck region at late stages in the fission process where there is an excess of neutrons.

Neutron emission between saddle point and scission has been explained by Fuller[50] as being due to a nonadiabatic potential change occurring in the nucleus during the fission process. On a one-dimensional model the nuclear potential well is supposed to be divided into two parts by a rising potential peak and it is shown that this would be expected to throw out of the nucleus a fraction of the nucleons. The fraction would only be zero for a very slow (adiabatic) potential rise. Fuller shows that an entirely reasonable risetime of the dividing potential can account for the pre-scission neutron emission observed by Bowman *et al.* Using Fuller's model, MacDonald[51] has shown that the probability of pre-scission neutron emission tends to rise with nuclear excitation, for constant risetime of the dividing potential. However, the major difficulty in applying Fuller's model is that this potential is treated as externally applied and it is difficult to see what alteration one should make in the rapidity of the process and in the residual nuclear excitation to simulate increased initial excitation.

In this discussion the attempts to understand the shape of the $\bar{\nu}$ function have been hampered by the paucity of fission data in the region of real interest, 0 to 6 MeV. At higher energies the competing $(n,n'f)$ reaction confuses results by intermixing an unknown fraction of fissions at low excitation. It appears that a systematic study of fission properties in the limited energy region below 6 MeV is required before any reliable interpretation can be placed on the shape of the $\bar{\nu}$-energy relationship presented here.

[49] L. Marquez, Proc. Phys. Soc. (London) **A70**, 546 (1957).
[50] R. W. Fuller, Phys. Rev. **126**, 684 (1962); and New York Operations Office Report No. 2962, 1962 (unpublished).
[51] N. MacDonald (private communication).

ACKNOWLEDGMENTS

We wish to express our appreciation for permission to include, prior to publication, the experimental results of Dr. J. C. Hopkins and Dr. B. C. Diven; Dr. I. Asplund-Nilsson, Dr. H. Condé, and Dr. N. Starfelt; and of D. W. Colvin and Dr. M. G. Sowerby. We are grateful to J. B. Parker, Dr. K. Parker, and Dr. A. Mercer for assistance with the solution of certain problems; and to H. Bird who has organized the necessary computations. Our thanks are due to Al Muggleton, H. Waller, and Dr. G. S. Perry for making certain of the fissile foils and targets used in this experiment; the tritium targets were supplied by RCC Amersham. The Van de Graaff operating team, led by V. Shepherd and later by G. James has given us excellent service under sometimes difficult conditions. E. R. Culliford and L. F. Pain have rendered untiring experimental assistance throughout this project. We are grateful to R. Batchelor for his interest in this work and to Professor K. W. Allen under whose guidance these experiments were begun.